

## Electrostatic solitary structures in presence of non-thermal electrons and a warm electron beam on the auroral field lines

S. V. Singh, G. S. Lakhina, R. Bharuthram, and S. R. Pillay

Citation: *Phys. Plasmas* **18**, 122306 (2011); doi: 10.1063/1.3671955

View online: <http://dx.doi.org/10.1063/1.3671955>

View Table of Contents: <http://pop.aip.org/resource/1/PHPAEN/v18/i12>

Published by the [American Institute of Physics](#).

---

### Related Articles

Numerical investigation of auroral cyclotron maser processes

*Phys. Plasmas* **17**, 056501 (2010)

Influence of suprathermal background electrons on strong auroral double layers: Observations

*Phys. Plasmas* **15**, 072901 (2008)

Intersystem collisional transfer of excitation in low altitude aurora

*J. Chem. Phys.* **78**, 2978 (1983)

Evidence that the electrostatic ion cyclotron instability is saturated by ion heating

*Phys. Fluids* **18**, 1590 (1975)

---

### Additional information on Phys. Plasmas

Journal Homepage: <http://pop.aip.org/>

Journal Information: [http://pop.aip.org/about/about\\_the\\_journal](http://pop.aip.org/about/about_the_journal)

Top downloads: [http://pop.aip.org/features/most\\_downloaded](http://pop.aip.org/features/most_downloaded)

Information for Authors: <http://pop.aip.org/authors>

### ADVERTISEMENT



**HAVE YOU HEARD?**

Employers hiring scientists  
and engineers trust  
**physicstodayJOBS**



<http://careers.physicstoday.org/post.cfm>

# Electrostatic solitary structures in presence of non-thermal electrons and a warm electron beam on the auroral field lines

S. V. Singh,<sup>1,2</sup> G. S. Lakhina,<sup>1</sup> R. Bharuthram,<sup>3</sup> and S. R. Pillay<sup>2,a)</sup>

<sup>1</sup>Indian Institute of Geomagnetism, Navi Mumbai, India

<sup>2</sup>School of Physics, University of Kwazulu-Natal, Durban, South Africa

<sup>3</sup>University of the Western Cape, Bellville, South Africa

(Received 5 September 2011; accepted 7 November 2011; published online 29 December 2011)

Electrostatic solitary waves (ESWs) have been observed by satellites in the auroral region of the Earth's magnetosphere. These ESWs are found to be having both positive and negative electrostatic potentials. Using the Sagdeev pseudo-potential technique, arbitrary amplitude electron-acoustic solitary waves/double layers are studied in an unmagnetized plasma consisting of non-thermally distributed hot electrons, fluid cold electrons, a warm electron beam, and ions. The inertia of the warm electrons, and not the beam speed, is essential for the existence of positive potential solitary structures. Existence domains for positive as well as negative potential electrostatic solitons/double layers are obtained. For the typical auroral region parameters, the electric field amplitude of the negative potential solitons is found to be in the range  $\sim(3-30)$  mV/m and  $\sim(5-80)$  mV/m for the positive potential solitons. For the negative potential solitons/double layers, the amplitudes are higher when their widths are smaller. On the other hand, the amplitude of the positive potential structures increase with their widths. © 2011 American Institute of Physics. [doi:10.1063/1.3671955]

## I. INTRODUCTION

Satellite observations have shown presence of electrostatic solitary waves (ESWs) in several regions of the Earth's magnetosphere, e.g., the auroral region,<sup>1-9</sup> plasma sheet boundary layer (PSBL),<sup>10</sup> the bow shock,<sup>11</sup> magnetopause, and on the cusp field lines<sup>12,13</sup> and magnetosheath.<sup>14-16</sup> These small scale, large amplitude ESWs which are bipolar or tripolar in nature can have either positive or negative potentials and are observed in the parallel electric field. Their electric field amplitudes can be a few mV/m in the PSBL to a few 100 mV/m in dayside auroral zone and even more in the auroral kilometric radiation (AKR) source region.<sup>17</sup> The velocities of these structures can be from  $\sim$  a few hundred to a few thousand km s<sup>-1</sup> and parallel scale sizes are  $\sim 100-1000$  m. These ESWs are generally associated with electron or/and ion beams.<sup>9,18-20</sup>

Theoretical models based on multi-component plasmas have been developed in the past to explain the solitary waves with negative potentials observed by Viking satellite in the Earth's magnetosphere.<sup>3-5,21-24</sup> However, these models could not explain the positive potential solitons. Several authors<sup>25-28</sup> studied the electron-acoustic solitons in four-component plasma and showed that depending upon the beam velocity, temperature, and density, solitons with positive polarity could be generated. We may emphasize that the solitons have no net potential drop across the structure whereas double layers are like the electrostatic shocks: both are associated with a net potential drop across the structure.<sup>29</sup>

It has been pointed out by Verheest *et al.*<sup>30</sup> that positive potential electron-acoustic solitons can be generated even without the electron-beam component, provided the hot

electron inertia is retained in the analysis. Kakad *et al.*<sup>31</sup> studied the coexistence of rarefactive and compressive electron-acoustic solitary waves for some specific plasma parameters in a four-component unmagnetized plasma system consisting of cold background electrons, a cold electron beam, and two types of ion species, i.e., cold and hot ions having Boltzmann distributions. Recently, Ghosh *et al.*<sup>32</sup> studied electron-acoustic solitary waves in a four-component magnetized plasma consisting of warm electrons, warm electron beam, and two types of hot ions. It was found that the characteristics and existence domain of the positive potential solitons is controlled by the ion temperature and concentration.

Lakhina *et al.*<sup>33</sup> studied ion and electron acoustic solitary waves in a three-component plasma system consisting of cold and hot electrons and one type of ions. For a given set of parameters, the critical Mach numbers for the ion-acoustic solitons are found to be smaller than those for electron-acoustic solitons. On the other hand, the ion-acoustic solitons had positive potentials for the parameters considered whereas the electron-acoustic solitons could have either positive or negative potentials depending on whether the fractional cold electron density with respect to the ion density was greater or less than a certain critical value. Further, the above study was extended by introducing a second ion species, i.e., a hot ion beam in the system and the hot electrons as having a beam component.<sup>34</sup> Three types of solitary waves, namely, slow ion-acoustic, ion-acoustic, and electron-acoustic solitons are found provided the Mach numbers exceed the critical values. Results of the model were applied to ESWs observed in the plasma sheet boundary layer. Small amplitude electron-acoustic solitary waves in an unmagnetized plasma consisting of cold plasma electrons and isothermal ions with two different temperatures have been studied by Kakad *et al.*<sup>35</sup> They showed the existence of

<sup>a)</sup>Deceased.

both positive and negative electrostatic potentials with bipolar pulses. It was also pointed out that the presence of cold electron beams and the hot electron inertia is not a necessary condition for the generation of compressive solitons as long as there are two temperature (low and high) ions along with cold plasma electrons in a plasma system. More recently, Lakhina *et al.*<sup>36,37</sup> developed a mechanism for generation of electrostatic electron-acoustic solitary waves and double layers using a four-component model consisting of core electrons, two counter-streaming electron beams and one type of ions. The model can explain the electrostatic solitary waves in the Earth's magnetosheath region observed by Cluster. The estimates of the electric field, pulse duration, and propagation speeds of the solitary structures are in good agreement with the observed bipolar pulses.

Most of the above studies on the solitary waves are based on the models using Boltzmann distribution function for electrons/ions or having fluid dynamical approach for all the species. However, in the Earth's magnetosphere, energetic electrons with non-thermal particle distributions have been observed. For example, Cairns *et al.*<sup>38</sup> used non-thermal distribution of electrons to study the ion-acoustic solitary structures observed by the FREJA satellite. It was shown that both compressive as well as rarefactive solitons could exist. Singh and Lakhina<sup>22</sup> studied the electron-acoustic solitary waves in an unmagnetized plasma consisting of non-thermally distributed electrons, fluid cold electrons and ions using the Sagdeev pseudo-potential technique. They found that the presence of non-thermal electrons modifies the parametric region where electron acoustic solitons can exist. Gill *et al.*<sup>39</sup> studied the small amplitude electron-acoustic solitary wave with cold and non-thermal electrons and ions.

It must be pointed out that all the above studies on electron acoustic solitary waves have either considered Boltzmann distribution for hot electrons along with the electron beam or nonthermal distribution for hot electrons without the electron beam. Therefore, in this paper, we present a general analysis for the electron-acoustic solitary waves/double layers in a four-component, unmagnetized plasma consisting of cold electrons, hot nonthermal electrons, and beam electrons and ions. This paper extends the work of Singh and Lakhina<sup>22</sup> by including an electron beam in the analysis. ***We must emphasize that our model deals with the time stationary state of the plasma system when the plasma instabilities, if excited initially by the electron beam, have been saturated. In a sense, the model deals with the nonlinear modes of the system.*** The existence domains for positive as well as negative potential electron acoustic solitons/double layers are obtained. The effect of various parameters such as particle density, beam velocity, nonthermality is studied on the evolution of electron acoustic solitary waves/double layers. In Sec. II, formulation of the model is presented, numerical results are presented in Sec. III and results are summarized in Sec. IV.

## II. FORMULATION

We consider a homogeneous, unmagnetized four component plasma consisting of non-thermal hot electrons, fluid

cold electrons, an electron beam, and ions. The non-thermal distribution for the hot electrons is given by Cairns *et al.*<sup>38</sup>

$$f_{0h}(v) = \frac{N_{0h}}{\sqrt{2\pi v_{th}^2}} \frac{\left(1 + \frac{\alpha v^4}{v_{th}^4}\right)}{(1 + 3\alpha)} \exp\left(-\frac{v^2}{2v_{th}^2}\right), \quad (1)$$

where  $N_{0h}$ ,  $v_{th} = \sqrt{T_h/m_e}$ ,  $m_e$ , and  $T_h$  are the equilibrium density, thermal speed, mass and temperature of the hot electrons, respectively, and  $\alpha$  is a parameter which determines the population of energetic non-thermal electrons. The distribution of electrons in the presence of non-zero potential can be found by replacing  $\frac{v^2}{v_{th}^2}$  by  $\frac{v^2}{v_{th}^2} - \frac{2e\Phi}{T_h}$ , where  $\Phi$  is the integration over the resulting distribution function gives the following expression for the hot electron density<sup>22,38</sup>

$$n_h = n_{0h}(1 - \beta\phi + \beta\phi^2)\exp(\phi), \quad (2)$$

and the other governing equations of the model are given by

$$\frac{\partial n_j}{\partial t} + \frac{\partial}{\partial x}(n_j v_j) = 0, \quad (3)$$

$$\frac{\partial v_j}{\partial t} + v_j \frac{\partial v_j}{\partial x} + \frac{1}{\mu_j n_j} \frac{\partial P_j}{\partial x} - \frac{Z_j}{\mu_j} \frac{\partial \phi}{\partial x} = 0, \quad (4)$$

$$\frac{\partial P_j}{\partial t} + v_j \frac{\partial P_j}{\partial x} + 3P_j \frac{\partial v_j}{\partial x} = 0, \quad (5)$$

$$\frac{\partial^2 \phi}{\partial x^2} = n_h + n_b + n_c - n_i, \quad (6)$$

where  $j = c, b, i$  represents cold electrons, beam electrons and ions, respectively,  $Z_j = \pm 1$  for electrons and ions, respectively, and  $\mu_j = m_j/m_e$ ,  $\beta = \frac{4\alpha}{(1+3\alpha)}$ . It must be pointed out that Eqs. (2)–(6) are normalized equations. We have normalized the densities by total electron density,  $N_0 = N_{0c} + N_{0h} + N_{0b} = N_{0i}$ , velocities by thermal speed of hot electrons,  $v_{th} = \sqrt{T_h/m_e}$ , lengths by effective hot electron Debye length defined as  $\lambda_{dh} = \sqrt{T_h/4\pi N_0 e^2}$ , temperature by hot electron temperature  $T_h$ , time by inverse of electron plasma frequency  $\omega_{pe}^{-1} = \sqrt{m_e/4\pi N_0 e^2}$ , the potential by  $T_h/e$ , and the thermal pressure by  $N_0 T_h$ . Here, we have used the adiabatic equation of state (cf. Eq. (5)) for the cold electrons, beam electrons, and ions with adiabatic index  $\gamma = 3$ .

In order to study the properties of arbitrary amplitude electrostatic solitary waves, we transform the above set of Eqs. (2)–(6) to a stationary frame moving with velocity  $V$ , the phase velocity of the wave, i.e.,  $\xi = (x - Mt)$ , where  $M = V/v_{th}$  is the Mach number ( $V$  is normalized with respect to the hot electron thermal speed). Then, we solve for perturbed densities using Eqs. (2)–(5) and substitute these expressions in the Poisson equation (6). Assuming appropriate boundary conditions for the localized disturbances along with the conditions that  $\phi = 0$ , and  $d\phi/d\xi = 0$  at  $\xi \rightarrow \pm\infty$ , we obtain the following energy integral,

$$\frac{1}{2} \left(\frac{d\phi}{d\xi}\right)^2 + V(\phi, M) = 0, \quad (7)$$

where  $V(\phi, M)$  is the Sagdeev potential given by

$$\begin{aligned}
 V(\phi, M) = & n_{0h} \left\{ 1 + 3\beta - (1 + 3\beta - 3\beta\phi + \beta\phi^2)e^\phi \right\} + n_{0c} \left[ M^2 - \frac{M}{\sqrt{2}} \left\{ M^2 + 3\sigma_c + 2\phi \pm \sqrt{(M^2 + 3\sigma_c + 2\phi)^2 - 12\sigma_c M^2} \right\}^{\frac{1}{2}} \right] \\
 & + n_{0c}\sigma_c \left[ 1 - 2\sqrt{2}M^3 \left\{ M^2 + 3\sigma_c + 2\phi \pm \sqrt{(M^2 + 3\sigma_c + 2\phi)^2 - 12\sigma_c M^2} \right\}^{-\frac{3}{2}} \right] \\
 & + n_{0b} \left[ (M - v_{0b})^2 - \frac{(M - v_{0b})}{\sqrt{2}} \left\{ (M - v_{0b})^2 + 3\sigma_b + 2\phi \pm \sqrt{\{(M - v_{0b})^2 + 3\sigma_b + 2\phi\}^2 - 12\sigma_b(M - v_{0b})^2} \right\}^{\frac{1}{2}} \right] \\
 & + n_{0b}\sigma_b \left[ 1 - 2\sqrt{2}(M - v_{0b})^3 \left\{ (M - v_{0b})^2 + 3\sigma_b + 2\phi \pm \sqrt{\{(M - v_{0b})^2 + 3\sigma_b + 2\phi\}^2 - 12\sigma_b(M - v_{0b})^2} \right\}^{-\frac{3}{2}} \right] \\
 & + \mu_i \left[ M^2 - \frac{M}{\sqrt{2}} \left\{ M^2 + \frac{3\sigma_i}{\mu_i} - \frac{2\phi}{\mu_i} \pm \sqrt{\left( M^2 + \frac{3\sigma_i}{\mu_i} - \frac{2\phi}{\mu_i} \right)^2 - \frac{12\sigma_i M^2}{\mu_i}} \right\}^{\frac{1}{2}} \right] \\
 & + \sigma_i \left[ 1 - 2\sqrt{2}M^3 \left\{ M^2 + \frac{3\sigma_i}{\mu_i} - \frac{2\phi}{\mu_i} \pm \sqrt{\left( M^2 + \frac{3\sigma_i}{\mu_i} - \frac{2\phi}{\mu_i} \right)^2 - \frac{12\sigma_i M^2}{\mu_i}} \right\}^{-\frac{3}{2}} \right], \tag{8}
 \end{aligned}$$

where  $\mu_j = m_j/m_e$ ,  $\sigma_j = T_j/T_h$ , and  $v_{0b}$  is the normalized electron beam speed. The first term on the right hand side (rhs) of Eq. (8) represents the hot electron contribution to the Sagdeev potential. In the absence of non-thermal electrons, i.e., for  $\alpha = \beta = 0$ , the term reduces to usual Boltzmann distributed hot electron contribution.<sup>21,23</sup> The second and third terms on the rhs of Eq. (8) represent the cold electron contribution and the next two terms are due to beam electrons. The last two terms on the rhs of Eq. (8) give the contribution of ions to the Sagdeev potential. It must be pointed out here that ion response is kept for the sake of completeness. It does not have any significant effect on the high frequency solitary/double layer structures for the parameters considered for numerical computation. To solve Eq. (8), one has to choose the positive (+) or negative (-) sign appearing in various terms on the rhs of this equation very carefully as these expressions are related to the square of the densities of the  $j$ th species. In order that the associated densities attain their undisturbed values in the limit of  $\phi \rightarrow 0$  at  $\xi \rightarrow \pm\infty$ , we must use the positive (+) sign when the condition  $(M - v_{0j})^2 + \frac{2\phi}{\mu_j} > \frac{3\sigma_j}{\mu_j}$  is satisfied, and the negative (-) sign when  $(M - v_{0j})^2 + \frac{2\phi}{\mu_j} < \frac{3\sigma_j}{\mu_j}$  is satisfied.<sup>36,40</sup>

### III. NUMERICAL RESULTS

Equation (7) describes the motion of a pseudo particle of unit mass in a pseudo-potential  $V(\phi, M)$  where  $\phi$  and  $\xi$  play the role of displacement  $x$  from the equilibrium and time, respectively. In the case of solitons, the pseudo particle is reflected in the pseudo-potential field at some  $\phi = \phi_0$  and returns to its initial state of  $\phi = 0$  with a zero potential drop. However, for the double layers, due to an additional condition of charge neutrality at  $\phi = \phi_0$ , the pseudo particle cannot be

reflected as both the pseudo-force and pseudo-velocity vanish there; instead it goes to another state with a net potential drop. Therefore, for soliton solutions of Eq. (7), the Sagdeev potential  $V(\phi, M)$  must satisfy the following conditions:  $V(\phi, M) = 0$ ,  $dV(\phi, M)/d\phi = 0$ ,  $d^2V(\phi, M)/d\phi^2 < 0$  at  $\phi = 0$ ,  $V(\phi, M) = 0$  at  $\phi = \phi_0$  ( $\phi_0$  is the maximum amplitude), and  $V(\phi, M) < 0$  for  $0 < |\phi| < |\phi_0|$ . For double layer solutions, an additional condition  $dV(\phi, M)/d\phi = 0$  at  $\phi = \phi_0$  should be satisfied.

From Eq. (8), it can be seen that Sagdeev potential  $V(\phi, M)$  and its first derivative with respect to  $\phi$  vanish at  $\phi = 0$ . On the otherhand, the condition  $d^2V(\phi, M)/d\phi^2 < 0$  at  $\phi = 0$  is satisfied provided  $M > M_0$ , where  $M_0$  is the critical Mach number satisfying the equation

$$\begin{aligned}
 f(M_0) \equiv & \frac{n_{0c}}{M_0^2 - 3\sigma_c} + \frac{n_{0b}}{(M_0 - v_{0b})^2 - 3\sigma_b} + \frac{1}{\mu_i M_0^2 - 3\sigma_i} \\
 & - n_{0h}(1 - \beta) = 0. \tag{9}
 \end{aligned}$$

Equation (9) has six roots but all the roots will not be physical. Therefore, we will consider only the real positive roots for  $M_0$ .

Figure 1 shows the existence curve for the electron-acoustic solitons/double layers with respect to normalized cold electron density,  $n_{0c}$ . Y-axis on the right hand side (rhs) shows the scale for Mach numbers (critical Mach number,  $M_0$  and maximum Mach number  $M_{max}$ ). Y-axis on the left hand side (lhs) shows the scale for the maximum electric potential amplitude,  $\phi_0$ . For each value of the  $n_{0c}$  and other parameters,  $M_0$  is obtained by solving the Eq. (9). From then onwards, we keep on increasing value of Mach number  $M$  until soliton/double layers solutions cease to exist. The value of largest Mach number,  $M$  beyond which soliton/double

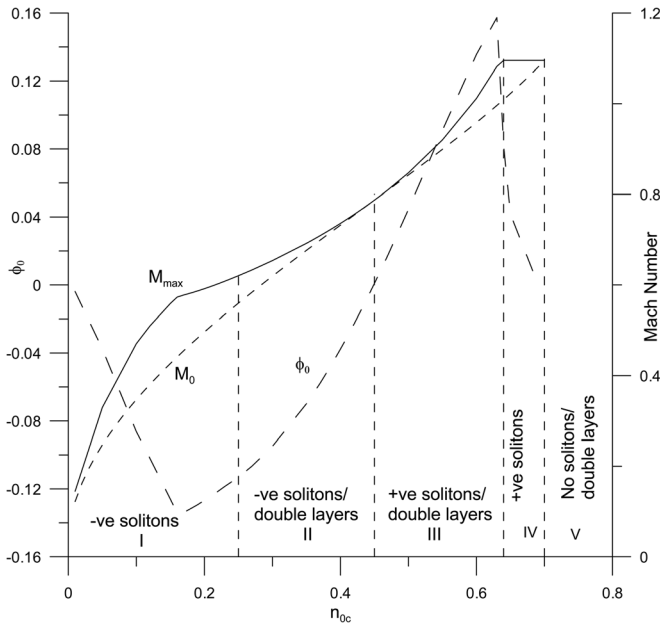


FIG. 1. Shows the existence curve for the electron-acoustic solitons/double layers with respect to normalized cold electron density,  $n_{0c}$ . Y-axis on the right hand side (rhs) shows the scale for Mach numbers (critical Mach number,  $M_0$  (dashed curve) and maximum Mach number  $M_{max}$  (solid curve)). Y-axis on the left hand side (l.h.s.) shows the scale for the maximum electric potential amplitude,  $\phi_0$  (long-dashed curve). The normalized plasma parameters are, hot electron density  $n_{0h} = 0.3$ , electron beam speed,  $v_{0b} = 0$ , ratio of beam to hot electron temperatures,  $\sigma_b = T_b/T_h = 0.4$ , ratio of cold to hot electron temperatures,  $\sigma_c = T_c/T_h = 0.001 = \sigma_i = T_i/T_h$  (ratio of ion to hot electron temperatures), and non-thermal parameter  $\alpha = 0$ .

layer solutions do not exist is known as  $M_{max}$  and the corresponding electric potential amplitude is  $\phi_0$ .

The chosen fixed parameters are, hot electron density  $n_{0h} = 0.3$ , electron beam speed,  $v_{0b} = 0$ , ratio of beam to hot electron temperatures,  $\sigma_b = T_b/T_h = 0.4$ , ratio of cold to hot electron temperatures,  $\sigma_c = T_c/T_h = 0.001 = \sigma_i = T_i/T_h$  (ratio of ion to hot electron temperatures), and non-thermal parameter  $\alpha = 0$ . Quasi-neutrality condition  $n_{0c} + n_{0h} + n_{0b} = 1$  is used to calculate the beam electron density. The existence domains of solitons and double layers are identified clearly with the dashed vertical lines. The maximum ( $M_{max}$ ) and minimum ( $M_0$ ) Mach numbers are represented by solid and dashed curves, respectively. The maximum electric potential amplitude ( $\phi_0$ ) is represented by long-dash curve. Numerical results of the investigation show only negative potential solitons for cold electron density,  $n_{0c} \leq 0.25$  and for  $0.25 \leq n_{0c} \leq 0.44$  negative potential solitons/double layers appear. Transition from negative solitons/double layers to positive solitons/double layers takes place at  $n_{0c} = 0.45$ . Positive potential solitons and double layers are seen for  $0.45 \leq n_{0c} \leq 0.63$ . Again, only positive potential soliton appear for  $0.64 \leq n_{0c} \leq 0.69$ . It is interesting to note that positive potential solitons disappear at cold electron density,  $n_{0c} = 0.7$ ; at this point, there are no beam electrons left in the plasma system. Thus, in order to have positive potential electron-acoustic solitary waves, an additional electron species with finite temperature and inertia is necessary and not the finite electron beam speed.

In Figure 1, regions I, II, III, IV, and V are identified with negative potential solitons, negative potential solitons and

double layers, positive potential solitons and double layers, and positive potential solitons and no solitons/double layers, respectively. From Figure 1, it is clear that maximum electric potential amplitude  $\phi_0$  first increases with the increase in cold electron density in the region I (negative potential solitons) and then decreases. In region II (negative potential solitons and double layers) and region IV (positive potential solitons), the maximum amplitude  $\phi_0$  decreases with the increase in cold electron density. In region III (positive potential solitons and double layers),  $\phi_0$  increases with the increase in cold electron density. Also, it noticed that the range of Mach numbers for which soliton/double layer solutions are obtained widens for regions I and III and narrows down in regions II and IV with increasing cold electron density,  $n_{0c}$ .

Next, we have carried out the numerical computations for the electron-acoustic solitary structures observed by Viking satellite and described by Dubouloz *et al.*<sup>5</sup> in detail. They have analyzed two events which are named as burst ‘‘a’’ and burst ‘‘b’’. The normalized plasma parameters for burst ‘‘a’’ are as follows: cold electron density  $n_{0c} = 0.143$ , hot electron density  $n_{0h} = 0.571$ , beam electron density  $n_{0b} = 0.286$ , ratio of beam to hot electron temperatures,  $\sigma_b = T_b/T_h = 0.2$  and ratio of cold to hot electron temperatures  $\sigma_c = T_c/T_h = 0.02 = \sigma_i (= T_i/T_h)$  (ratio of ion to hot electron temperatures). In our computations, we have taken electron beam speed,  $v_{0b} = 0$  and non-thermal parameter  $\alpha = 0.0$ . The results of the computation shows that only electron-acoustic solitary waves with negative potential can be generated for these parameters. The soliton solution exists for  $0.43 \leq M \leq 0.462$  for the above parameters. Similar results are obtained for the burst ‘‘b’’ parameters where  $n_{0c} = 0.074$ ,  $n_{0h} = 0.556$ , and  $n_{0b} = 0.37$  and other parameters are the same as for burst ‘‘a’’. The results are consistent with our findings described in the previous paragraph. The results of the analysis of burst ‘‘a’’ are shown in Figure 2 for various mach numbers as shown on the curves.

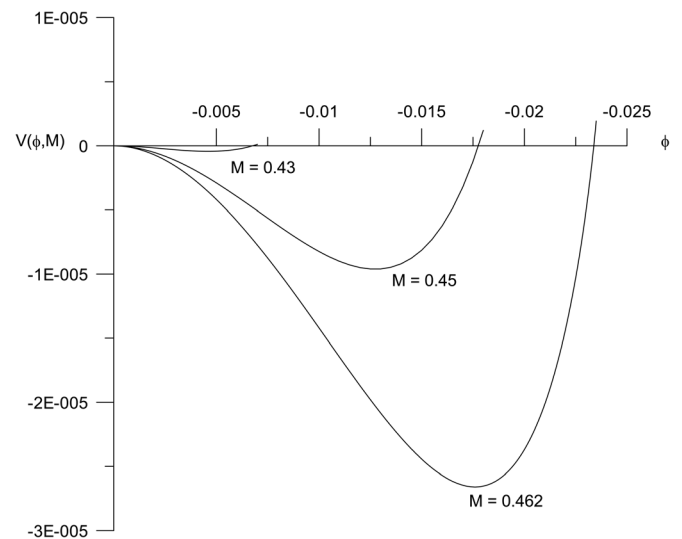


FIG. 2. Sagdeev potential,  $V(\phi, M)$  versus normalized potential  $\phi$  for various Mach numbers as shown on the curves. The normalized plasma parameters of burst ‘‘a’’ are:  $n_{0c} = 0.143$ ,  $n_{0h} = 0.571$ ,  $n_{0b} = 0.286$ ,  $\sigma_b = T_b/T_h = 0.2$ , and  $\sigma_c = T_c/T_h = 0.02 = \sigma_i = T_i/T_h$ . Here, we have taken beam speed,  $v_{0b} = 0$  and non-thermal parameter  $\alpha = 0.0$ .

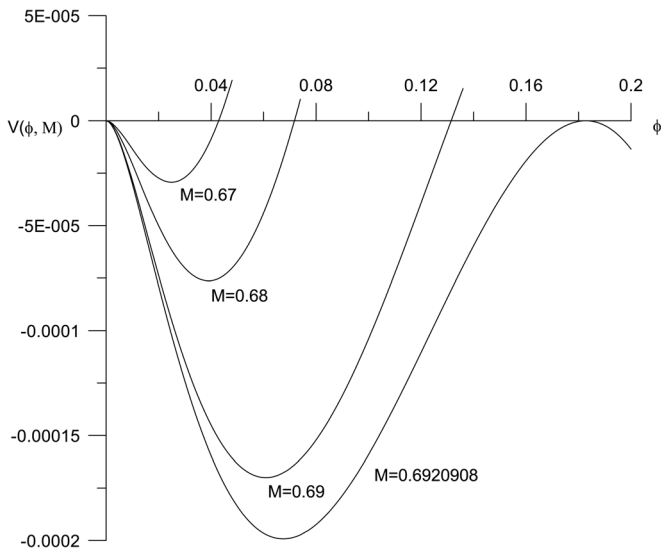


FIG. 3. Variation of Sagdeev potential  $V(\phi, M)$  with the normalized potential  $\phi$  for various mach numbers shown on the curves. Here,  $n_{0c} = 0.571$ ,  $n_{0h} = 0.143$ , and all other parameters are same as described in Figure 2. Note that we have swapped the cold electron density with hot electron density and positive potential electron-acoustic solitons and double layer can be seen.

In Figure 3, we have swapped the cold electron density with the hot electron density for the parameters of burst “a”, i.e., we have taken  $n_{0c} = 0.571$  and  $n_{0h} = 0.143$  and all other parameters are same as described in previous paragraph. For these parameters, positive potential solitons and double layers are obtained. This is exactly the case we have described in our parametric study in Figure 1. Positive potential structures are found for cold electron density being larger than the hot electron density in presence of additional warm electron component. The soliton solutions exist for  $M \geq 0.65$  with double layers appearing for  $M = 0.6920908$ .

Figure 4 shows the variation of Sagdeev potential  $V(\phi, M)$  versus the normalized electrostatic potential  $\phi$  for the parameters of burst “a” and Mach number,  $M = 0.46$ , electron beam speed,  $v_{0b} = 0.1$  for different values of nonthermal parameter,  $\alpha$  as shown on the curves. It should be noted that the electron-acoustic soliton amplitude decreases with the increase in nonthermality. These results are in agreement with findings of Singh and Lakhina (2004)<sup>22</sup> in a three-component plasma consisting of cold electrons, hot nonthermal electrons and ions. For  $v_{0b} > 0.174$ , soliton solutions are not found for the above mentioned parameters of the burst “a”.

Figure 5 shows the variation of Sagdeev potential,  $V(\phi, M)$  versus the normalized electrostatic potential  $\phi$  for the parameters of burst “a” for various values of the normalized electron beam speed,  $v_{0b}$  as shown on the curves. The other parameters are, Mach number,  $M = 0.46$  and nonthermal parameter  $\alpha = 0.1$ . It is clear from the figure that amplitude of the solitons decreases with increase of electron beam speed. The behaviour is similar to the results obtained by Singh *et al.*<sup>23</sup> in a four-component plasma of cold electron, hot Maxwellian electrons, beam electrons and ions. For  $\alpha > 0.146$ , soliton solutions are not found for the parameters of the burst “a”.

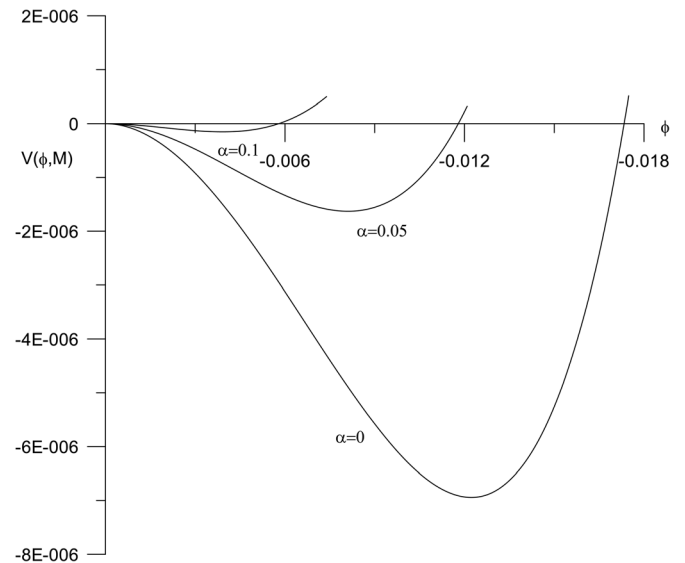


FIG. 4. Shows the variation of Sagdeev potential  $V(\phi, M)$  versus the normalized potential  $\phi$  for the parameters of burst “a” and Mach number,  $M = 0.46$ , electron beam speed,  $v_{0b} = 0.1$  for different values of nonthermal parameter,  $\alpha$  as shown on the curves.

#### IV. DISCUSSION

Properties of the electron-acoustic solitary waves in an unmagnetized four-component plasma consisting of cold electrons, hot nonthermal electrons, and warm beam electrons and ions have been examined. Present theoretical model is the extension of the model used by Singh and Lakhina<sup>22</sup> by including the beam electrons. The existence regime for the both negative and positive potential solitons and double layers has been examined. It is found that in order to have positive potential structures, electron beam velocity is not required but an additional warm electron component is necessary. It may be recalled that only negative potential structures could be found in the three-component plasma

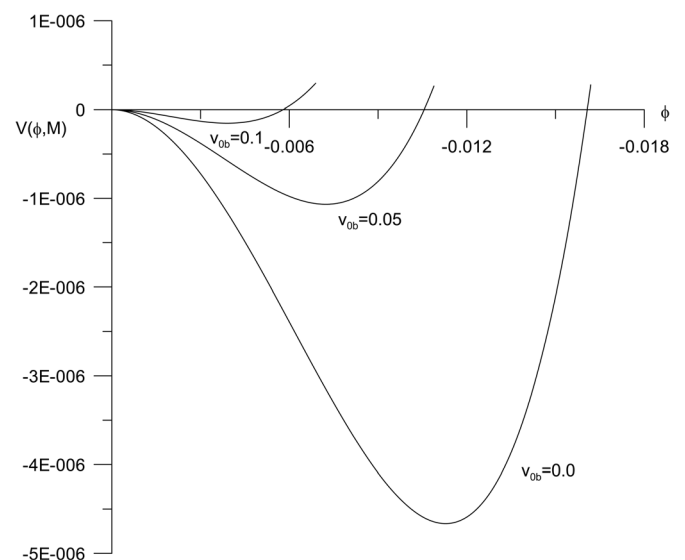


FIG. 5. Shows the variation of Sagdeev potential,  $V(\phi, M)$  versus the normalized potential  $\phi$  for the parameters of burst “a” for various values of the normalized electron beam speed,  $v_{0b}$  as shown on the curves. The other parameters are, Mach number,  $M = 0.46$  and nonthermal parameter,  $\alpha = 0.1$ .

model of Singh and Lakhina<sup>22</sup> consisting of fluid cold electrons and non-thermal, hot electrons and ions.

The effect of nonthermality is found to reduce the amplitude and widens the range of Mach numbers for which the nonlinear structures are obtained. The inclusion of nonthermal electrons pushes the minimum and maximum Mach numbers to the higher side for which nonlinear structures are obtained. The inclusion of an electron beam in the model does reduce the maximum amplitude of the electron-acoustic solitary waves and widens the range of Mach numbers for which soliton solutions are obtained. The range of Mach numbers is much wider as compared to the effect of nonthermality.

The electric field amplitudes, parallel widths, velocities, and time duration of the electron-acoustic solitons obtained by the model are in the range of  $\sim(3\text{--}30)$  mV/m,  $\sim(500\text{--}236)$  m,  $\sim(2855\text{--}3070)$  km s<sup>-1</sup>, and  $\sim(0.08\text{--}0.17)$  ms, respectively, for the burst “a” parameters. Here, we have taken  $\alpha = 0$ ,  $v_{0b} = 0$  and total electron density  $N_0 = 3.5$  cm<sup>-3</sup>, and hot electron temperature  $T_h = 250$  eV. Width of soliton decreases with increase in soliton amplitude. The observed value of the maximum electric field in the case of burst “a” is about 37 mV/m (cf. Table I of Ref. 5). Thus, our results are in good agreement of the Viking observations in the auroral region. However, we would like to point out that there is no direct observations of negative potential electron-acoustic-solitons. The observations show that ESWs have either positive or negative potentials. We are interpreting ESWs properties in terms of electron-acoustic solitons and double layers.

For the positive potential structures of Figure 3, the electric field amplitudes, parallel widths, velocities, and time duration of the electron-acoustic solitons obtained by the model are in the range of  $\sim(5\text{--}80)$  mV/m,  $\sim(500\text{--}2300)$  m,  $\sim(4317\text{--}4600)$  km s<sup>-1</sup>, and  $\sim(0.12\text{--}0.5)$  ms, respectively. These values are higher compared to the negative potential structures. Further, the width of the solitons increases with increase in soliton amplitude.

The recent observations of electron holes in the auroral regions connected to the plasma sheet boundary layer appear to be consistent with the generation of an electron acoustic instability. In these regions, the plasma consists of a cold electron population, hot electrons, and warm electron beams. Our theoretical model developed in this paper is in agreement with the observations.<sup>41</sup>

It must be emphasized here that positive potential solitary structures are observed along with the electron beams. Our theoretical results do point to a situation where positive potential solitary structures can be obtained in the presence of an additional warm beam electron-component along with the cold and hot electron-components. We have shown theoretically that positive potential structures do evolve with finite electron beam speed. However, it is not necessary for the warm electron component to have always a finite electron beam speed. This may seem in apparent disagreement with the observations. However, there is no disagreement in reality as our analysis is valid for the time stationary state when all the instabilities driven by the electron beam have been saturated. In this state, the beam velocity will always be

smaller than the threshold for the instability or can even be zero, but its effect is felt through an additional warm electron component.

## ACKNOWLEDGMENTS

S.V.S. would like to thank University of the Western Cape, Bellville, South Africa for the warm hospitality during his visit. S.V.S. also thanks the Department of Science and Technology, New Delhi, India for providing the financial support to attend the COSPAR 2008, Montreal, Canada and presenting the paper. G.S.L. would like to thank the Indian National Science Academy, New Delhi, India, for the support under the Senior Scientist scheme.

- <sup>1</sup>M. Temerin, K. Cerny, W. Lotko, and F. S. Mozer, *Phys. Rev. Lett.* **48**, 1175 (1982).
- <sup>2</sup>R. Bostrom, G. Gustafsson, G. Holback, G. Holmgren, H. Koskinen, and P. Kintner, *Phys. Rev. Lett.* **61**, 82 (1988).
- <sup>3</sup>N. Dubouloz, R. Pottellette, M. Malingre, G. Holmgren, and P. A. Lindqvist, *J. Geophys. Res.* **96**, 3565, doi:10.1029/90JA02355 (1991).
- <sup>4</sup>N. Dubouloz, R. Pottellette, M. Malingre, and R. A. Treumann, *Geophys. Res. Lett.* **18**, 155, doi:10.1029/90GL02677 (1991).
- <sup>5</sup>N. Dubouloz, R. A. Treumann, R. Pottellette, and M. Malingre, *J. Geophys. Res.* **98**, 17415, doi:10.1029/93JA01611 (1993).
- <sup>6</sup>F. S. Mozer, R. E. Ergun, M. Temerin, C. Cattell, J. Dombeck, and J. Wygant, *Phys. Rev. Lett.* **79**, 1281 (1997).
- <sup>7</sup>E. E. Ergun, C. W. Carlson, J. P. McFadden, F. S. Mozer, D. T. Delory, W. Peria, C. C. Chaston, M. Temerin, I. Roth, L. Muschietti, R. Elphic, R. Strangeway, R. Pfaff, C. A. Cattell, D. Klumppar, E. Shelley, W. Peterson, E. Moebius, and L. Kistler, *Geophys. Res. Lett.* **25**, 2041, doi:10.1029/98GL00636 (1998).
- <sup>8</sup>B. T. Tsurutani, J. K. Arballo, G. S. Lakhina, C. M. Ho, B. Buti, J. S. Pickett, and D. A. Gurnett, *Geophys. Res. Lett.* **25**, 4117, doi:10.1029/1998GL900114 (1998).
- <sup>9</sup>S. R. Bounds, R. F. Pfaff, S. F. Knowlton, F. S. Mozer, M. A. Temerin, and C. A. Kletzing, *J. Geophys. Res.* **104**, 28709, doi:10.1029/1999JA900284 (1999).
- <sup>10</sup>H. Matsumoto, H. Kojima, T. Miyatake, Y. Omura, M. Okada, I. Nagano, and M. Tsutsui, *Geophys. Res. Lett.* **21**, 2915, doi:10.1029/94GL01284 (1994).
- <sup>11</sup>S. D. Bale, P. J. Kellogg, D. E. Larson, R. P. Lin, K. Goetz, and R. P. Lepping, *Geophys. Res. Lett.* **25**, 29292932 (1998).
- <sup>12</sup>J. R. Franz, P. M. Kintner, and J. S. Pickett, *Geophys. Res. Lett.* **25**, 1277, doi:10.1029/98GL50870 (1998).
- <sup>13</sup>C. Cattell, J. Dombeck, J. R. Wygant, M. K. Hudson, and F. S. Mozer, *Geophys. Res. Lett.* **26**, 425, doi:10.1029/1998GL900304 (1999).
- <sup>14</sup>J. S. Pickett, J. D. Menietti, D. A. Gurnett, B. T. Tsurutani, P. M. Kintner, E. Klatt, and A. Balogh, *Nonlinear Processes Geophys.* **10**, 311 (2003).
- <sup>15</sup>J. S. Pickett, L.-J. Chen, S. W. Kahler, O. Santolk, M. L. Goldstein, B. Lavraud, P. M. E. Decreau, R. Kessel, E. Lucek, G. S. Lakhina, B. T. Tsurutani, D. A. Gurnett, N. Cornilleau-Wehrin, A. Fazakerley, H. R'eme, and A. Balogh, *Nonlinear Processes Geophys.* **12**, 181193 (2005).
- <sup>16</sup>J. S. Pickett, L.-J. Chen, R. L. Mutel, I. H. Christopher, O. Santolik, G. S. Lakhina, S. V. Singh, R. V. Reddy, D. A. Gurnett, B. T. Tsurutani, and E. Lucek, *Adv. Space Res.* **41**, 1666–1676 (2008).
- <sup>17</sup>R. Pottellette, R. E. Ergun, R. A. Truemann, M. Berthomier, C. W. Carlson, J. P. McFadden, and I. Roth, *Geophys. Res. Lett.* **26**, 2629, doi:10.1029/1999GL900462 (1999).
- <sup>18</sup>Y. Omura, H. Kojima, and H. Matsumoto, *Geophys. Res. Lett.* **21**, 2923, doi:10.1029/94GL01605 (1994).
- <sup>19</sup>Y. Omura, H. Kojima, N. Miki, T. Mukai, H. Matsumoto, and R. Anderson, *J. Geophys. Res.* **104**, 14627, doi:10.1029/1999JA900103 (1999).
- <sup>20</sup>N. Singh, *Nonlinear Processes Geophys.* **10**, 53 (2003).
- <sup>21</sup>R. L. Mace, S. Baboolal, R. Bharuthram, and M. A. Hellberg, *J. Plasma Phys.* **45**, 323 (1991).
- <sup>22</sup>S. V. Singh and G. S. Lakhina, *Nonlinear Processes Geophys.* **11**, 275 (2004).
- <sup>23</sup>S. V. Singh, R. V. Reddy, and G. S. Lakhina, *Adv. Space Res.* **28**, 1643 (2001).

- <sup>24</sup>S. G. Tagare, S. V. Singh, R. V. Reddy, and G. S. Lakhina, *Nonlinear Processes Geophys.* **11**, 215 (2004).
- <sup>25</sup>M. Berthomier, R. Pottelle, M. Malingre, and Y. Khotyaintsev, *Phys. Plasmas* **7**, 2987 (2000).
- <sup>26</sup>M. Berthomier, R. Pottelle, L. Muschietti, I. Roth, and C. W. Carlson, *Geophys. Res. Lett.* **30**, 2148, doi:10.1029/2003GL018491 (2003).
- <sup>27</sup>R. L. Mace and M. A. Hellberg, *Phys. Plasmas* **8**, 6 (2001).
- <sup>28</sup>W. F. El-Taibany, *J. Geophys. Res.* **110**, A01213, doi:10.1029/2004JA010525 (2005).
- <sup>29</sup>R. Pottelle, R. A. Treumann, M. Berthomier, and J. Jasperse, *Nonlinear Processes Geophys.* **10**, 87 (2003).
- <sup>30</sup>F. Verheest, T. Cattart, and M. A. Hellberg, *Space Sci. Rev.* **121**, 299 (2005).
- <sup>31</sup>A. P. Kakad, S. V. Singh, R. V. Reddy, G. S. Lakhina, S. G. Tagare, and F. Verheest, *Phys. Plasmas* **14**, 052305 (2007).
- <sup>32</sup>S. S. Ghosh, J. S. Pickett, G. S. Lakhina, J. D. Winningham, B. Lavraud, and P. M. E. Decreau, *J. Geophys. Res.* **113**, A06218, doi:10.1029/2007JA012768 (2008).
- <sup>33</sup>G. S. Lakhina, A. P. Kakad, S. V. Singh, and F. Verheest, *Phys. Plasmas* **15**, 062903 (2008).
- <sup>34</sup>G. S. Lakhina, S. V. Singh, A. P. Kakad, F. Verheest, and R. Bharuthram, *Nonlinear Processes Geophys.* **15**, 903 (2008).
- <sup>35</sup>A. P. Kakad, S. V. Singh, R. V. Reddy, S. G. Tagare, and G. S. Lakhina, *Adv. Space Res.* **43**, 1945 (2009).
- <sup>36</sup>G. S. Lakhina, S. V. Singh, A. P. Kakad, M. L. Goldstein, A. F. Vi nas, and J. S. Pickett, *J. Geophys. Res.* **114**, A09212, doi:10.1029/2009JA014306 (2009).
- <sup>37</sup>G. S. Lakhina, S. V. Singh, A. P. Kakad, and J. S. Pickett, *J. Geophys. Res.* **116**, A10218, doi:10.1029/2011JA016700 (2011).
- <sup>38</sup>R. A. Cairns, A. A. Mamun, R. Bingham, R. Dendy, R. Bostrom, C. M. C. Nairns, and P. K. Shukla, *Geophys. Res. Lett.* **22**, 2709, doi:10.1029/95GL02781 (1995).
- <sup>39</sup>T. S. Gill, H. Kaur, and N. S. Saini, *Chaos, Solitons Fractals* **30**, 10201024 (2006).
- <sup>40</sup>F. Verheest, M. A. Hellberg, and I. Kourakis, *Phys. Plasmas* **15**, 112309 (2008).
- <sup>41</sup>R. Pottelle, *J. Geophys. Res.* **116**, A00K12, doi:10.1029/2010JA016192 (2011).